MODELLING BLAST WAVE CLEARING USING LOAD_BLAST_CLEARING: PART I – VERIFICATION AND VALIDATION

Written by:
L. Schwer[1], S. Rigby[2] and T. Slavik[3]
[1]**Schwer Engineering & Consulting Services, USA**
[2]**University of Sheffield, UK**
[3]**Ansys, Inc., USA**

1 Introduction

An engineering model of air blast has been a useful feature in LS-DYNA since implemented by Randers-Pehrson and Bannister [1], based on the industry standard ConWep [2] engineering air blast model. In addition to the ConWep above ground and surface burst incident and reflected pressure histories, Randers-Pehrson and Bannister introduced a reduction in pressure magnitude due to oblique blast waves. This implementation is known by the keyword Load_Blast and has remained unchanged until about 2011.

Several improvements were made to the Load_Blast keyword, under the new keyword Load_Blast_Enhanced. The main enhancements included:

- Multiple explosions (bombs);
- Two new forms of blast waves; moving air bursts and height-of-burst Mach Stem blast waves;
- Graphics capability via LS-PrePost to allow fringing pressures and pressure history assessment.

Recently, additional improvements were made via the new keyword Load_Blast_Clearing that works with Load_Blast_Enhanced. This allows the inclusion of finite target boundaries and the pressure reduction that may occur due to pressure relief (clearing) from these free edges. Use is made of an analytical blast wave clearing method developed by Hudson [3] to modify the reflected surface pressures on finite targets.

The purpose of the present manuscript is to introduce the new keyword Load_Blast_Clearing, to provide some verification and validation, and explore a novel application involving oblique blast waves.

The manuscript has three main sections and an appendix:

1. Verification & Validation using an independent implementation of Hudson's method and a series of small-scale experimental results;
2. Using Multi-Material ALE solver to supplement the available validation data via:
   - Additional target locations including the target edges;
   - Calculate the reduction in target impulse when clearing is included in a simulation;
   - Assess the effect of target obliquity on Load_Blast_Clearing results.
3. Clearing effects on deformable targets - Validation.

2 Verification and validation - Load_Blast_Clearing

Tyas *et al*. [4] presented a series of blast loaded targets with three free edges allowing for "clearing" of the pressure throughout the interior surface of the targets. Clearing begins at free edges where the discontinuity between adjoining reflecting surfaces and transmitting open-air allows a rapid reduction of the reflected pressure. The reduction in reflected pressure propagates away from the edge, thus reducing the pressure history relative to loading for an infinite wall. Typically, the associated reduction in target impulse due to clearing is small, and most often neglected in blast analyses.

3 Experiments and data

Figure 1 illustrates the blast loaded face of the target and pressure gauge locations. A 20 mm steel plate was mounted on the surface of a similarly dimensioned large concrete block forming an essentially rigid target. The target is loaded by the blast from a 250 g PE4 (nominally similar to C4) hemispherical surface charge placed at even numbered distances between 4 and 10 meters away; the 4 m results are the focus in the present manuscript as the results are similar at the other charge ranges. Two repeatable tests were performed at each range; at the 4 m range the difference in maximum impulse from Test 1 to Test 2 was only 2% for both gauge locations.

Figure 2 shows the pressure and impulse histories for the two gauges with the 250 g PE4 hemispherical surface charge at the 4 m range. The difference in maximum impulse is about 10% between the two gauges.

The easiest way to understand the effects of clearing is to compare the pressure and impulse data to the corresponding results for an infinite target, i.e. using LS-DYNA Load_Blast_Enhanced with a 300 g TNT equivalent hemispherical charge (equivalence of 1.2 assumed by Tyas *et al*. [4]) Figure 3 compares the pressure histories from gauges G1 & G2 with the corresponding Load_Blast_Enhanced results at G1. Note: there is only a slight difference in time of arrival and maximum pressure between the two-gauge locations when using Load_Blast_Enhanced and those small differences are not significant in explaining the effects of clearing.

The differences in the two measured pressure histories and the Load_Blast_Enhanced history are due to the relative distances of the two gauges from free edges. Gauge G2 is the closest to a free edge, i.e. top surface 168.75 mm away, and the pressure begins to decrease about 0.5 ms after time of arrival (TOA); 7.66 ms. The pressure at the center gauge G1, 337.5 mm from the target top, begins to decrease at about 1.0 ms after TOA; 8.06 ms. Very soon after, the clearing from the symmetric lateral edges, 355 mm away, further reduces the pressure at both gauges. Note: at a nominal acoustic speed for the relief waves of 340 m/s, the times of 0.5 and 1.0 ms are confirmed for these free edge distances.

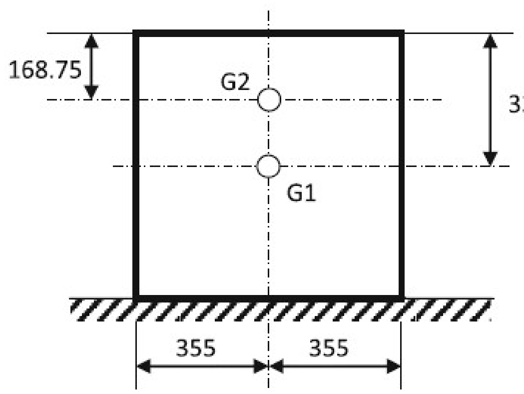

Figure 1 Illustration of target and pressure gauge locations (Figure 4 in Tyas *et al*. [4])

The positive pressure phase at both gauges ends at about 1.5 ms after TOA, i.e. 8.5 ms, about a full 1.25 ms before the corresponding positive phase duration for the Load_Blast_Enhanced pressure history. The termination of the positive phase corresponds to the time of maximum impulse. The effect of clearing is to reduce the maximum impulse (not shown) from the Load_Blast_Enhanced baseline by about a 20% and 30% at gauges G1 and G2, respectively.

4 Engineering model for blast clearing

Both Tyas *et al*. [4] and Bogosian *et al*. [5] use the blast clearing engineering model of Hudson [3] for comparison with the same Tyas *et al*. experimental data. Additionally, Tyas *et al*. compare results with another engineering model of clearing they refer to as ConWep [2] "Loads on Structures" (LoS) and Bogosian *et al*. provide comparisons with UFC 3-340-02 [6] and a set of guidelines published by ASCE [7].

Recently, Slavik [8] implemented the Hudson clearing method in LS-DYNA under the keyword LOAD_BLAST_CLEARING (LBC). The initial implementation is restricted to simple blast loaded targets such as the target used in the above experiments by Tyas *et al*. It is the purpose of this manuscript to compare this LS-DYNA implementation with the Hudson results presented by both Tyas *et al*.

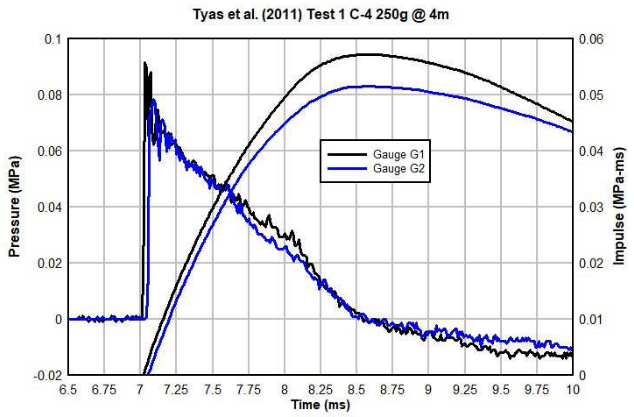

Figure 2 Comparison of measured pressure and corresponding impulse histories at the two gauge locations for the 4 m charge range

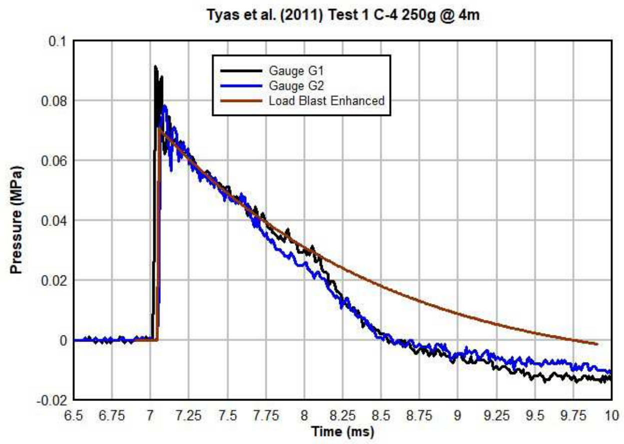

Figure 3 Comparison of measured pressure histories with corresponding results from Load_Blast_Enhanced

and Bogosian *et al*., that are identical, as part of a verification effort; comparing the LBC results to the experimental data is part of a subsequent validation effort.

Additionally, Rigby [9] provided a digital version of the Hudson clearing results for the Tyas *et al*. experiments. These digital results, see Figure 4, differ slightly from the Hudson results in Tyas *et al*. Figures 5 & 6 and Bogosian *et al*. Figure 12. The differences occur in how the symmetric target lateral side relief waves arrive at the centerline gauges. Rigby developed a rule-of-thumb to not "double account" for these symmetric relief waves as was previously the case, and this was seen to better match the experiments.

The LS-DYNA new keyword *LOAD_BLAST_CLEARING works in conjunction with *LOAD_BLAST_ENHANCED (LBE) and requires minimal additional input consisting of the bomb ID and four node numbers indicating the four corners, and thus associated four edges, of the target subject to blast clearing. Note: the current implementation does not allow for the explicit inclusion of a ground surface, i.e. non-clearing edge. However, such a non-clearing edge can be effected by placing the corner nodes of that edge some distance below the ground surface, e.g. mirroring the height of the target below the ground surface. If such an edge is sufficiently far away, clearing will not occur during the time of interest in the simulation.

Figure 5 compares the measured pressure histories at gauges G1 and G2 and corresponding impulse histories with the Hudson clearing results from Rigby [9] and application of the LS-DYNA Load_Blast_Clearing Hudson method. At both gauge locations the two Hudson clearing implementations provide nearly identical results and track the data quite well. Differences between the pressure histories are more evident in the impulse histories.

At gauge G1 the two Hudson implementation maximum impulses are essentially equal and only slightly, about 5.5 and 6%, less than the data. For gauge G2, the LBC impulse deviates from the data, and Rigby Hudson implementation, when the relief wave from the top of the target arrives. The Rigby Hudson implementation impulse

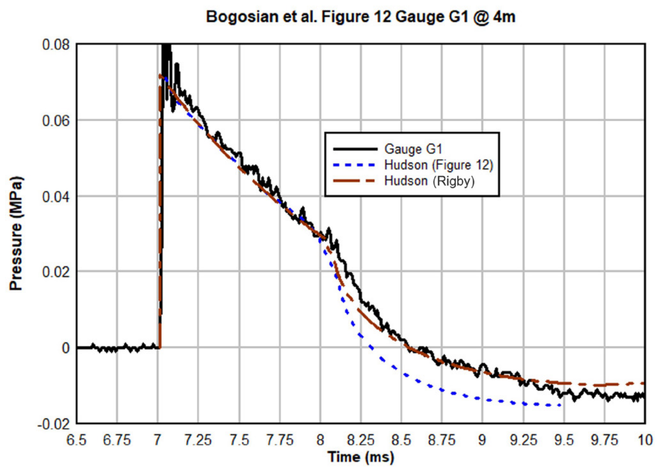

Figure 4 Comparison of Hudson clearing results from previous publications with results recently provided by Rigby [9]

begins to deviate from the data when the lateral relief waves arrive. Interestingly, both Hudson methods impulse histories again agree about 0.75 ms after the positive phase terminates.

5 Using an MM-ALE model to investigate clearing

The LS-DYNA implementation of Hudson's clearing method is an engineering tool for assessing the effect of clearing on blast loaded targets. However, validating Hudson's method or assessing its limitations, depends on the availability of suitable experimental results. To date there is a limited set of validation quality experimental results designed to assess clearing. Most of these experiments are focused on flat targets with blast loads normal to the target, i.e. no significant angle of incidence. Also, the gauges tend to be along the vertical and horizontal centerlines of the target.

One possibility to expand the number and location of pressure gauge points for comparison with Hudson's method is via a validated MM-ALE air blast model. In such a model, the blast wave propagates through air and interacts with the target allowing the physics to

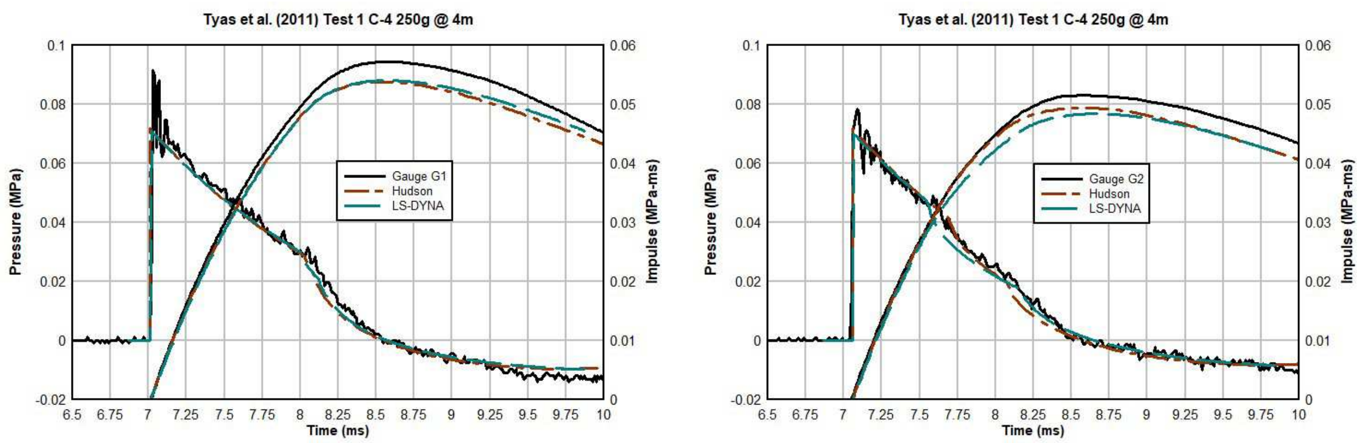

Figure 5 Comparison of the measured pressure and corresponding impulse histories at gauges G1 (left) and G2 (right) with the Hudson clearing method results from Rigby [9] and LS-DYNA LBC implementation

capture any clearing effects. This differs from the engineering approach associated with Load_Blast_Enhanced where the blast load is applied directly to the target and no clearing is modeled unless the keyword Load_Blast_Clearing is included in the model.

As shown in Figure 6, a symmetric MM-ALE model representing half the target in the Tyas *et al*. experiment was constructed using an air domain that is 500 mm larger than the target dimension. To further limit the air domain, a layer of elements in the direction of the bomb, i.e. the *z*-direction, are defined as ambient material where the Load_Blast_Enhanced incident pressure is applied. The blast wave then propagates through the air domain and is reflected off the block of MM-ALE material representing the target. Seven tracer particles are included in the model with two located at the experimental gauge locations, G1=T1, and G2=T5. Three tracers are placed on the target edges at the top (T4), right side (T3) and bottom (T7). The final two tracers are spaced 177.5 mm to right (T2) of the center gauge and 168.75 mm below (T6) the center gauge, i.e. midway points to the right and bottom edges, respectively. The model contains over 6 million hexahedra cubes of side length 5 mm; a 10 mm mesh discretization did not produce satisfactory pressure histories.

Figure 7 shows a comparison of the measured pressure histories at the two-gauge locations, and the corresponding impulse histories, with the results from the MM-ALE simulation. The easiest comparison among the results is via the impulse histories. The maximum impulses at the two-gauge locations, are slightly less, by 4.6 and 3.5%, respectively, than the corresponding values from the MM-ALE simulation. This comparison validates the MM-ALE model. Note: the decreasing pressure in the MM-ALE results after about 8.5 ms is due to the limited size of the air domain allowing additional nonphysical relief waves to arrive from the domain edges.

Finally, Figure 8 shows the comparison of the pressure and impulse histories from the two LS-DYNA simulation methods: MM-ALE and Load_Blast_Clearing. As with the MM-ALE comparison with the data, the MM-ALE maximum impulses are larger than the corresponding Load_Blast_Clearing impulse by about 10% for both gauge locations.

Table 1 provides a summary of the maximum impulse for the two gauges and the corresponding relative errors for Hudson's clearing method as implemented by Rigby [9], Load_Blast_Clearing and the MM-ALE solvers. Both implementations of Hudson clearing slightly underpredict the measured maximum impulses. The MM-ALE solver over predicts the maximum impulses by about the same relative error as the Hudson method under predictions.

6 Non-gauged locations

The MM-ALE solver can also provide pressure history results at other locations on the target that were not monitored with pressure gauges in the Tyas experiments. Some of these locations are the midpoints to the right (T2) and below (T6) the central gauge G1 and at the target edges, i.e. top (T4), right side (T3) and bottom (T7).

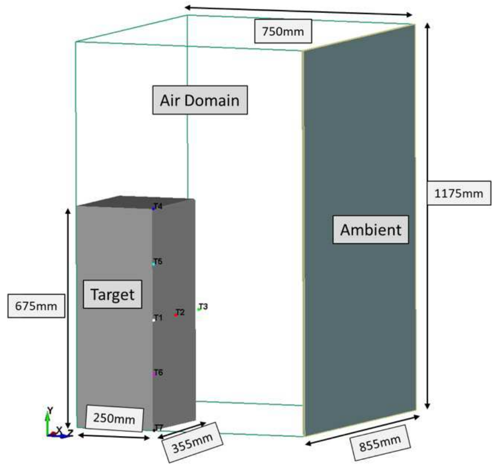

Figure 6 Illustration of the symmetric MM-ALE model of target and seven tracer locations

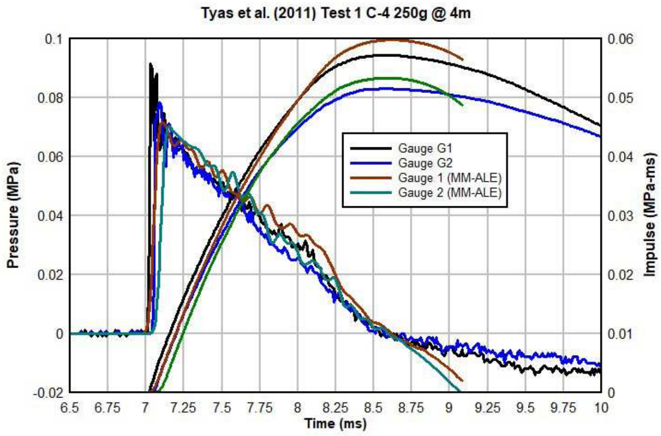

Figure 7 Comparison of measured pressure histories and corresponding impulse histories with the results from the MM-ALE model

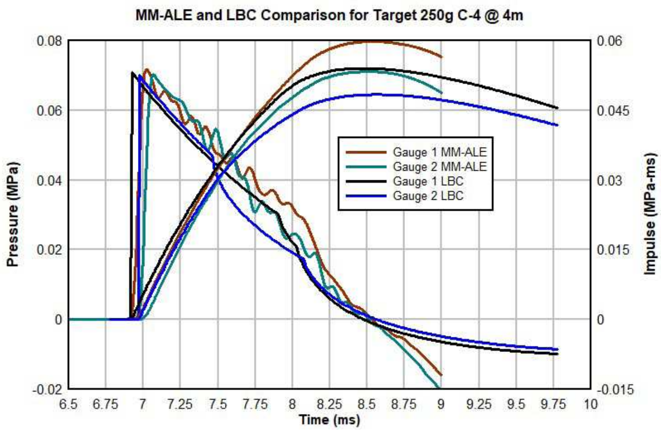

Figure 8 Comparison of pressure and impulse histories from the MM-ALE and Load_Blast_Clearing (LBC) simulations

	GAUGE 1	GAUGE 2
Data (Tyas)	**0.0571**	**0.0515**
Hudson (Rigby)	-0.060	-0.041
Hudson (LBC)	-0.054	-0.062
MM-ALE	0.047	0.035

Table 1 Comparison of maximum impulse relative errors

Figure 9 compares the Load_Blast_Clearing (dashed colored lines) and MM-ALE (black lines) results at the three edges of the target. At the top (T4) and right-side (T3) edges, the LBC maximum impulse exceeds that from the MM-ALE solver by about 23 and 18%, respectively. At the bottom (T7), the situation is reversed as the LBC does not account for the ground surface, so clearing effects are *included* in the LBC solution; the LBC solution underestimates the maximum impulse by about 33%. Note: clearing at the ground surface could have been avoided by defining that clearing edge to be farther below the target ground surface.

Figure 10 compares the Load_Blast_Clearing (dashed colored lines) and MM-ALE (black lines) results at two midpoints of the target, i.e. mid-right (T2) and mid-below (T6) of the center gauge. At the mid-right location, the LBC maximum impulse exceeds the corresponding MM-ALE value by about 19%. However, at the midpoint below the center gauge location, the MM-ALE impulse exceeds that of the LBC solver by about 21%. This is a direct consequence of the LBC solver not accounting for the ground surface and allowing clearing from the ground below to affect this location.

As mentioned previously, a work-around to include a ground (non-clearing) surface when using the LS-DYNA Load_Blast_Clearing keyword is to locate the non-reflecting edge a distance away from the target region. A supplemental LBC model was created with the bottom (ground) edge located half the target height (337.5 mm) below the nominal ground surface. The resulting maximum impulses values at the ground (T7) and mid-below (T6) locations were only 11% and 6%, less, respectively, than the MM-ALE maximum impulses. Figure 11 compares the MM-ALE pressure and impulse histories with the corresponding nominal LBC and extended depth (LBC-Deep) simulations.

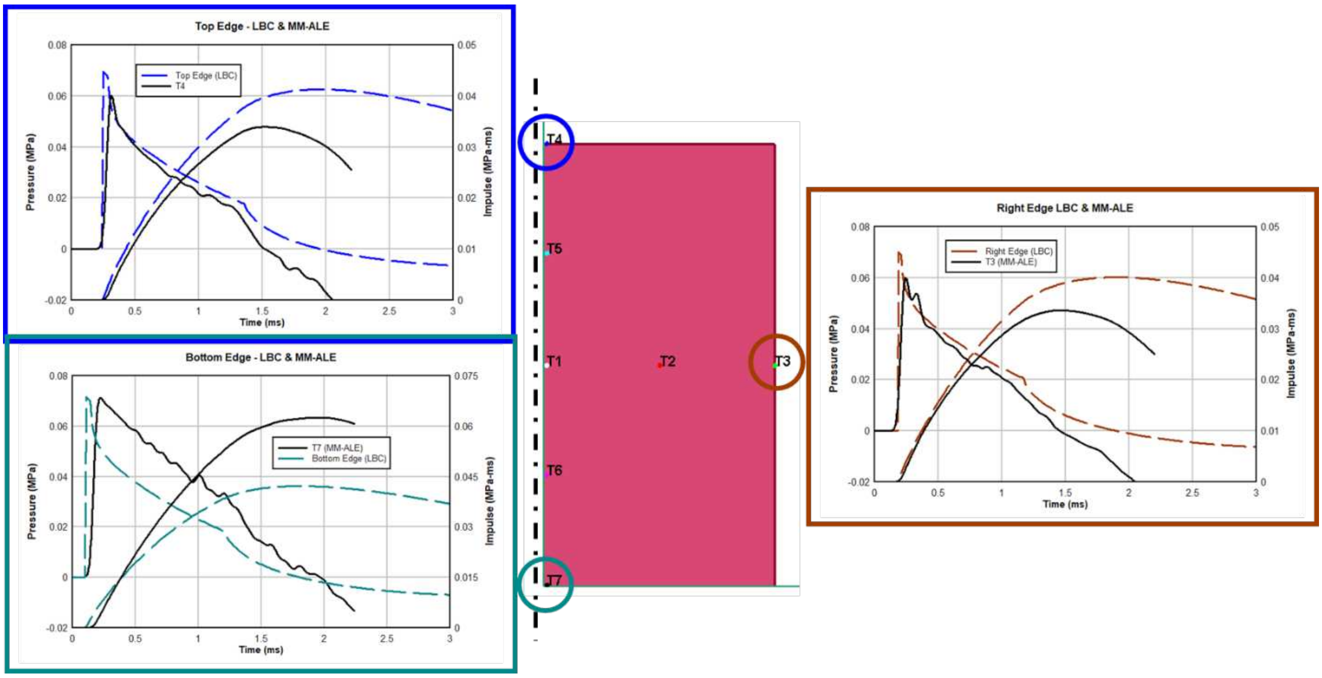

Figure 9 Comparison of pressure and impulse histories at the target edges from the LBC and MM-ALE solvers

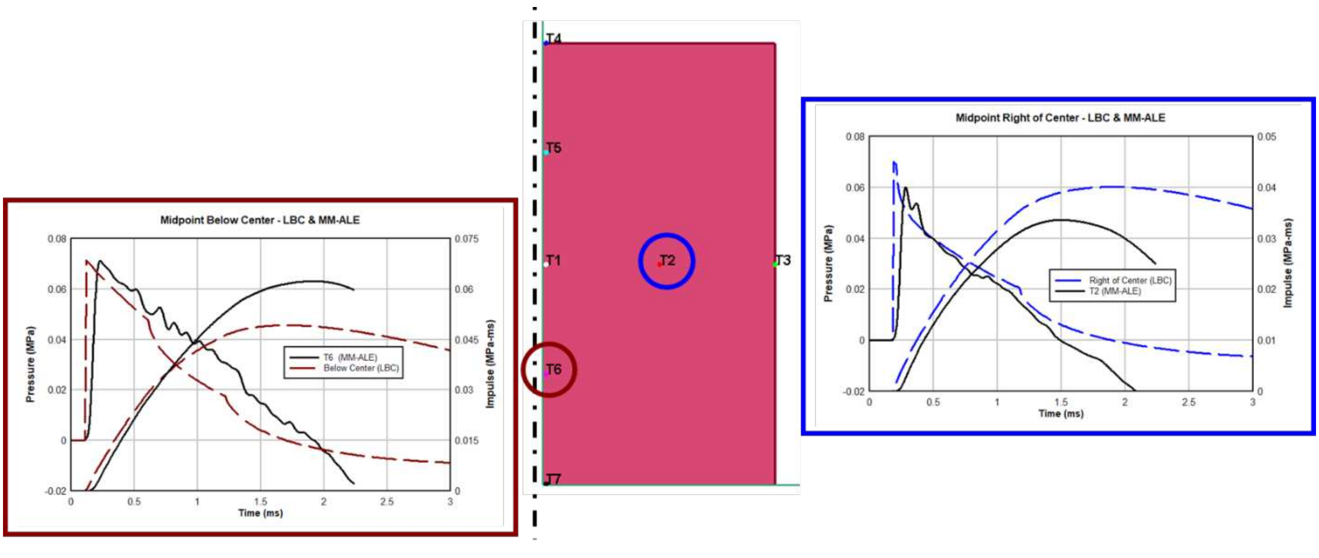

Figure 10 Comparison of pressure and impulse histories at the target midpoints to the right (T2) and below (T6) the center gauge from the LBC and MM-ALE solvers

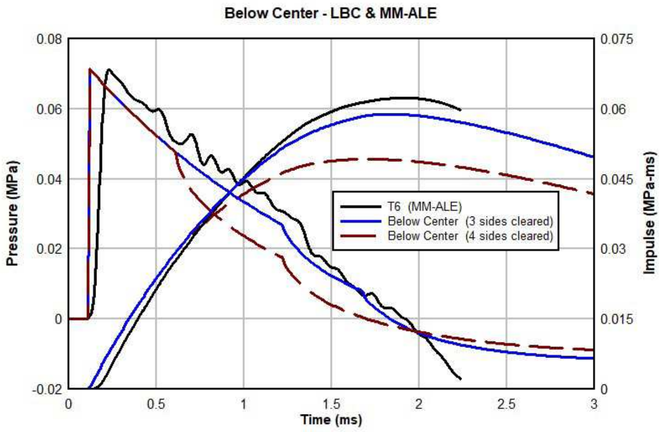

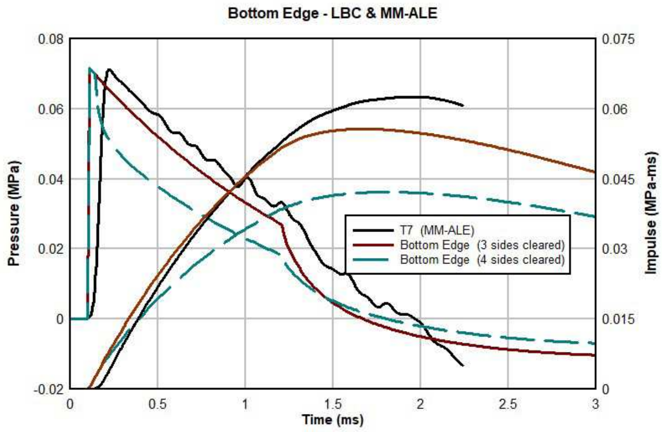

Figure 11 Comparison of pressure and impulse histories below center (left) and ground level (right) from MM-LAE and two LBC simulations

7 Target momentum and clearing

A global effect of clearing on a blast loaded target can be obtained by evaluating the total momentum of the target. The target surface described above, 675×710 mm, was made into an elastic aluminum plate with a thickness of 50 mm. The lateral sides and top remained free edges, i.e. clearing is active, while the bottom edge was prescribed to not allow clearing, i.e. the target's ground surface was maintained. Four case were simulated:

1. MM-ALE;
2. Load_Blast_Clearing (LBC) with 4 sides cleared (default implementation);
3. LBC with 3 sides cleared (no clearing from base of target);
4. Load_Blast_Enhanced (LBE) No clearing.

Figure 12 shows the momentum history comparison for the four cases with three significant times in the histories highlighted. The results comparisons are summarized as follows:

- The MM-ALE and the LBC with 3-sides cleared initially agree until about 1.17 ms when the MM-ALE switches to tracking the 4-side clearing LBC at 1.6 ms.
- The MM-ALE and the LBC default (4 sides cleared) have the same momentum up to 2.2 ms; the MM-ALE simulation is terminated at 2.2 ms because unloading from domain edges begins to influence the pressure histories.
- All three clearing results indicate a decrease in momentum after about 2.0 ms - negative phase of the pressure; see previously shown cleared pressure histories in Figure 9 through Figure 11.
- Without clearing (LBE) the momentum at 3ms is overestimated by about 45% with respect to the 4 sides cleared case.

Figure 13 attempts to compare fringes of velocity at the three significant times indicated in Figure 12. Note: velocity here is a surrogate for momentum as the mass is uniform across the target and the same for all cases. The velocity fringes range from a minimum (negative maximum) value of -0.4 m/s to -0.2 m/s. The two LBC cases can be compared directly and clearly indicate the difference in momentum for the 4 and 3-sided clearing cases. The MM-ALE results are included for completeness as it is difficult to compare the MM-ALE fringes to those from the LBC 3 sides cleared case, even though the total momentum agree.

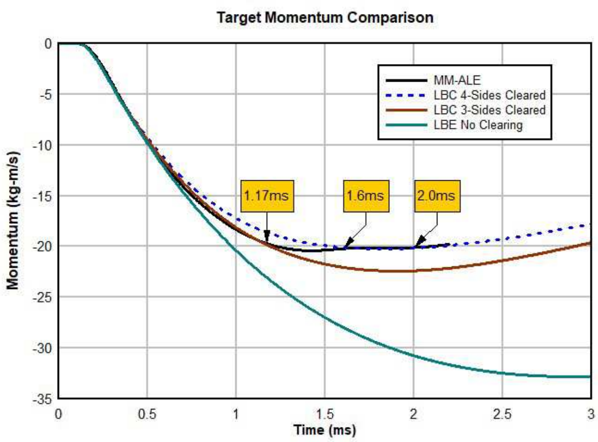

Figure 12 Comparison of target momentum from four models with and without clearing

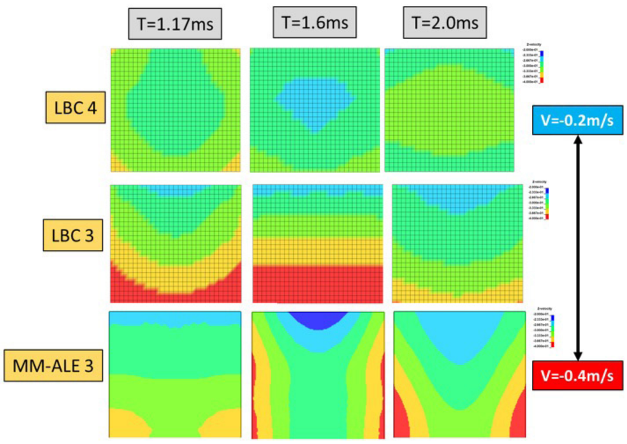

Figure 13 Fringes of through thickness velocity from three clearing models

8 Oblique blast wave clearing

The MM-ALE model also makes it possible to compare pressure histories for an oblique blast on a target. The same target as used previously, 675×335 mm as the vertically symmetric target, was rotated about the ground level by 20° such that the top edge is now 235 mm behind the bottom edge and 40 mm lower. The same 300 g equivalent TNT hemispherical ground charge was detonated 4 m in front of the target's bottom edge. The seven tracer particles shown previously in Figure 6 were also rotated 20° to remain in approximately the same relative position to the target as for the unrotated target, i.e. as if affixed to the face of the target. Similarly, the LBC model was rotated 20° and the blast loaded segments corresponding to the seven-tracer particles were used in the pressure history comparisons.

Figure 14 shows the comparison of pressures histories from the MM-ALE and LBC simulations for the points along the vertical centerline of the target, i.e. from top to bottom T5, T1, T6 and T7, respectively. Note: there is no pressure history comparison for the top of target location, i.e. T4, as the tracer particle only recorded ambient (0.1 MPa) pressure. It is speculated the angled target makes for zones of mixed (air and aluminum) cells since the target face cuts across the Cartesian Eulerian grid.

There is good agreement between the MM-ALE and LBC pressure and impulse histories for the four target locations shown as a side view in Figure 14. The agreement is best at the center of the target, T1, and just below the center at T6. Just above the target center, T5, the LBC pressure history arrives before (0.1 ms) the MM-ALE tracer with the converse late (0.13 ms) arrival at the bottom tracer T7. Also note at the T5 location, the effect of the unloading wave on the two pressure histories is opposite, i.e. the MM-ALE pressure increases after about 2.5 ms while the LBC pressure decreases after 2.35 ms.

Figure 15 is a front view of the target face showing the comparison of pressures histories from the MM-ALE and LBC simulations for the points along the horizontal centerline of the target, i.e. from centerline to outer edge T1, T2 and T3, respectively. Again, the center gauge location T1 indicates good agreement as does the gauge location to the immediate right, i.e. T2. The far-right edge gauge T3 indicates that the LBC unloads more slowly than the pressure from the MM-ALE simulation and hence the LBC over predicts the impulse at that edge.

9 Blast wave clearing effects on deformable plates

Rigby *et al*. [10] presented results for a set of blast loaded deformable targets with and without the inclusion of blast clearing effects. The deformable targets with clearing were embedded in a finite support block that had nearby free edges. Targets without clearing were embedded in an "infinite" wall. The goal was to measure the center displacement of the targets and compare the measured results with engineering model results with and without blast clearing.

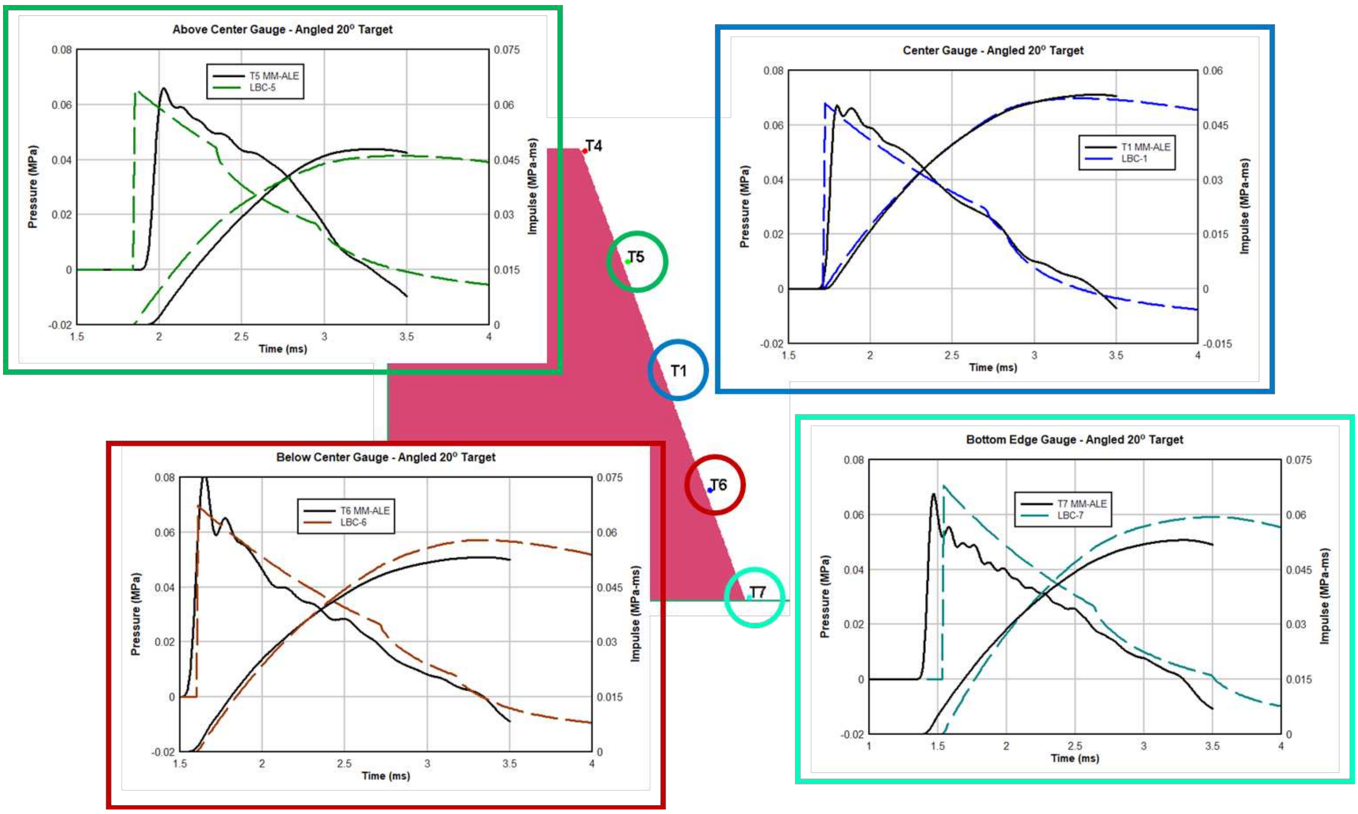

Figure 14 Oblique (20°) target MM-ALE and Load_Blast_Clearing comparisons of vertical centerline points (side view)

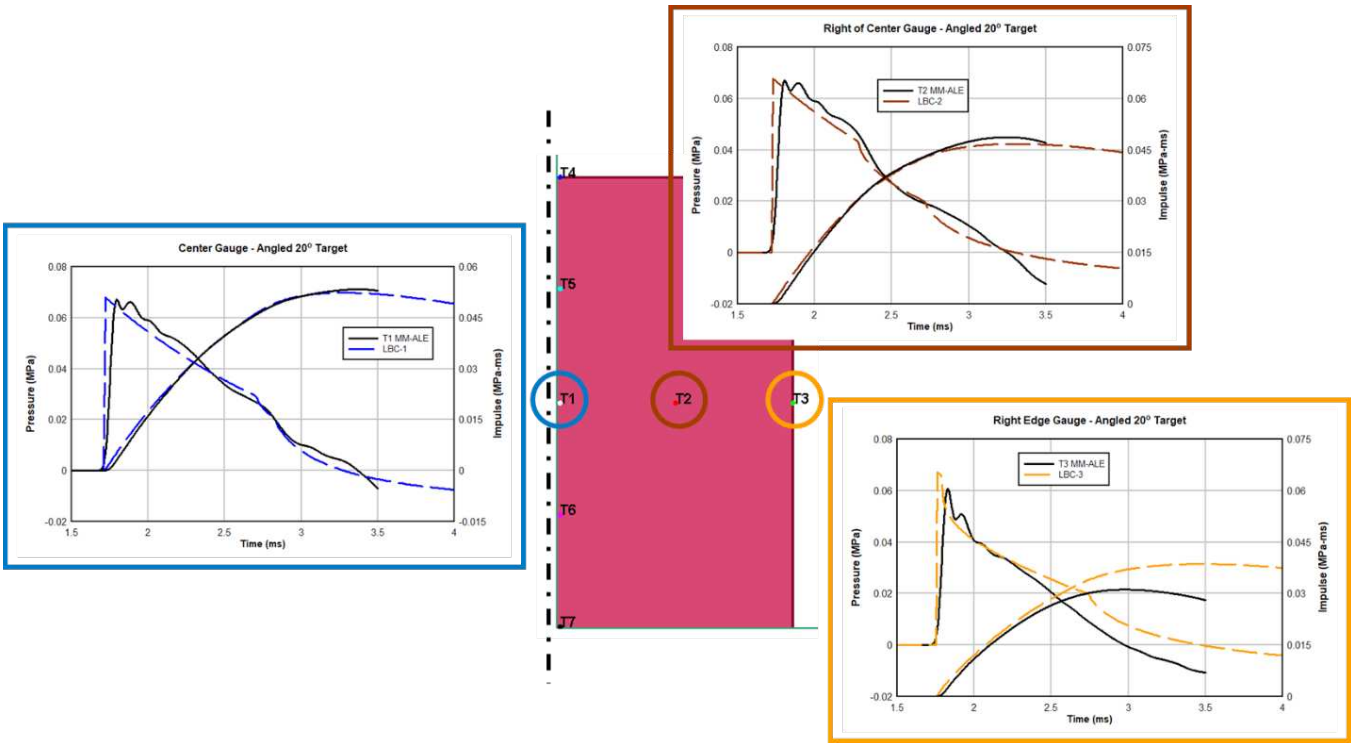

Figure 15 Oblique (20°) target MM-ALE and Load_Blast_Clearing comparisons of horizontal centerline points (front view)

10 Experiments and data

Figure 16 (left) is a plan view illustration of the experimental setup. A hemispherical explosive charge is placed on the surface equidistant from both targets. The finite target, Figure 16 (right), is a concrete block of facing surface dimensions 782×690 mm. Within the finite target is a thin (0.835 mm) steel plate of dimensions 320×305 mm fixtured over a cutout in the block such that the vertical edges are clamped and the horizontal (top & bottom) edges are free. A similarly constructed and fixtured plate is in the "infinite" extent of the bunker wall. Thus, two identical deformable targets are loaded by the same explosive charge only differing by the distances to free edges surrounding the plates.

The hemispherical surface PE4 charges used in the tests had masses ranging between 50 and 175 g. All charges were located at a range of 6 m from the target providing scaled distances between 15.3 and 10.1 m/kg when a factor of 1.2 is used to convert the PE4 mass to equivalent TNT mass. Two repeatable tests were performed for each charge mass with displacement histories at the center of the plates reported.

11 Modelling

The deformable plate was discretized with an array of 64×64 shell elements mimicking the discretization used by Rigby *et al*. The shell material was elastic steel and used five through thickness (0.835 mm) integration points. The plate's two vertical edges were constrained from rotation about the *y*-direction (vertical) and *z*-direction (through thickness) translation. This allowed the plate edges to move in plane in the two orthogonal *x*-*y* directions.

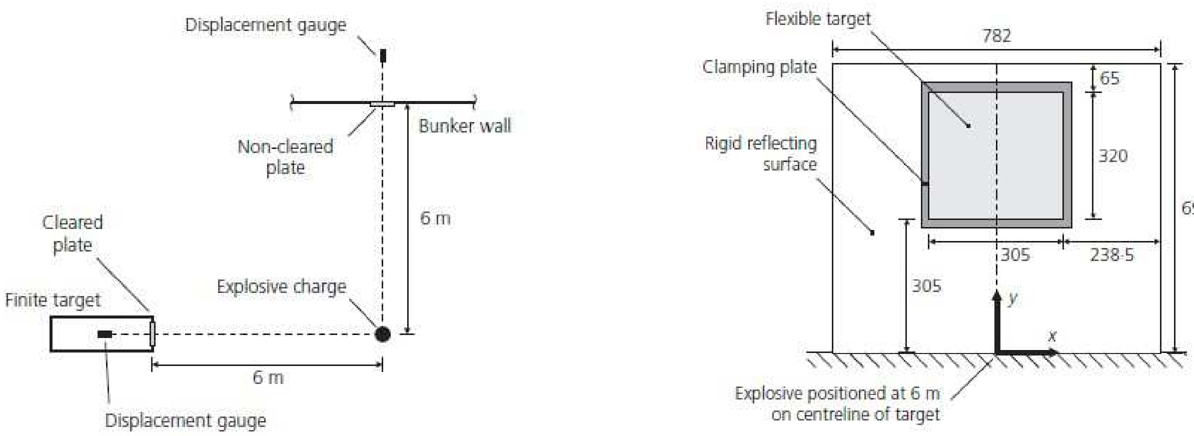

Figure 16 Illustration of experimental setup and details of target and finite block

The engineering blast model Load_Blast_Enhanced (LBE) was used to generate the plate loading. In the simulations where clearing was allowed, the additional keyword Load_Blast_Clearing (LBC) was activated.

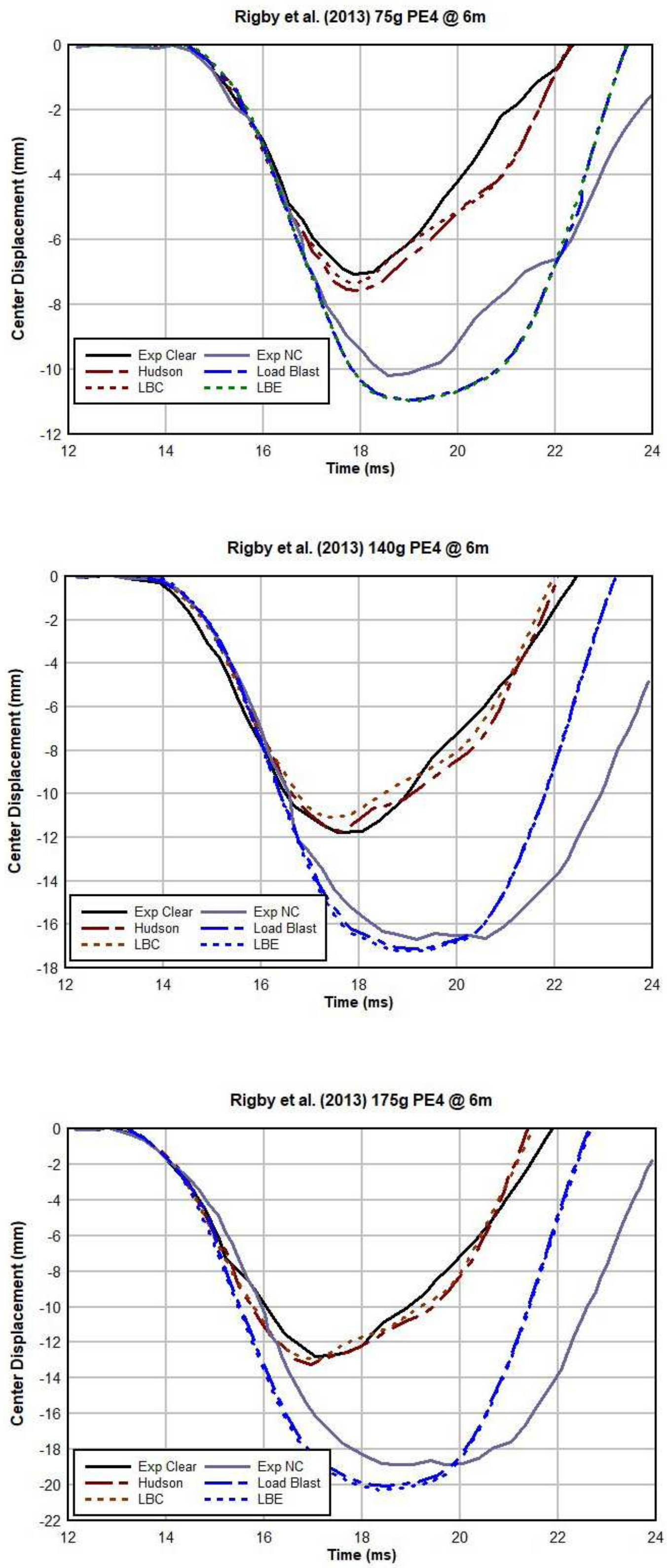

Figure 17 Experimental and numerical results for deformable plates subjected to cleared and non-cleared blast loads: top Test 4 (75 g); middle Test 8 (140 g); bottom Test 9 (175 g)

12 Results

Rigby *et al*. [10] report experimental and numerical results for three charge masses: 75, 140 and 175 g in their Figure 5. Those results and the corresponding present (LBE/LBC) center displacement results are provided in present Figure 17. For each of the three charge masses the data from Rigby *et al*. for the cleared and non-cleared case are shown. The experimental data are solid lines and Rigby *et al*. numerical results are long-and-short dashed lines. The corresponding LS-DYNA results from the present study are shown as small-dashed lines.

For the non-cleared cases, Rigby *et al*. used the older Load_Blast keyword while the present results used the more recent Load_Blast_Enhanced keyword. For this hemispherical surface loading, these two keywords produce identical results. Table 3 in Rigby *et al*. presents relative errors in maximum displacement for all tests and simulations. For the non-cleared tests shown here in Figure 17, i.e. Tests 4 (75 g), 8 (140 g) and 9 (175 g) these relative errors are 7%, 2% and 4%, respectively.

For the cleared cases, Rigby *et al*. used a MATLAB-based implementation of Hudson's [3] clearing method to generate cleared pressure histories at all nodal points. These were then applied to the shell model using LS-DYNA keywords Load_Node_Point and Define_Curve. As mentioned previously, the LS-DYNA cleared results in the present work were obtained by adding the new keyword Load_Blast_Clearing, also based on Hudson's clearing method. This keyword requires minimal additional input consisting of the bomb ID and four node numbers indicating the four corners, and thus associated four edges of the target subject to blast clearing. In this case the four corners of the concrete block face shown previously in Figure 16 (right).

In general, these two implementations of Hudson's clearing method provide similar results. The two methods also reproduce the experimental results well. Rigby *et al*. in Table 3 provides relative errors for the tests with clearing results shown here in Figure 17, i.e. Tests 4 (75 g), 8 (140 g) and 9 (175 g), of 6%, -1% and 5%, respectively.

The displacement comparisons shown here in Figure 17 demonstrate the difference in structural response when target clearing effects are included or ignored. The cleared targets have about 70% of the maximum displacement observed for the non-cleared targets.

13 Summary

The LS-DYNA implementation of Hudson's [3] clearing method for blast loaded targets has been shown to reproduce the independent implementation of Hudson's clearing by Tyas *et al*. [4], Bogosian *et al*. [5] and Rigby [9]. In addition to this verification, the LS-DYNA implementation also compares well with the experimental data provided by Tyas *et al*. [4].

Beyond verification and validation of the LS-DYNA Load_Blast_Clearing (LBC) feature, comparisons were presented with a multi-material arbitrary Lagrange Eulerian (MM-ALE) solution. The MM-ALE solver allowed for pressure and impulse comparisons at locations other than the two-gauge locations available from the Tyas *et al*. experiments. Edge locations at the top, side and bottom of the target face were compared. Except for the bottom edge, the LBC and MM-ALE results agreed. A better comparison of the bottom gauge results was obtained when the location of the bottom cleared edge was place well below the ground surface, i.e. affecting a non-cleared target edge.

An MM-ALE solution was generated for a blast wave impacting an oblique (20°) target. Again, the pressure and impulse results compared favorably with the exception the MM-ALE tracer located at the top of the target that only recorded ambient pressure. It is speculated that the angled target makes for zones of mixed (air and aluminum) cells since the target face cuts across the Cartesian Eulerian grid.

The experiments of Rigby *et al*. [10] were simulated to illustrate the structural effect of reduced pressure and impulse due to including blast wave clearing. These experiments included identical thin steel plates with finite and infinite lateral extents of the surrounding reflecting surfaces; the former includes clearing from the support edges and the latter does not. Center displacement were compared to both LBC with clearing and LBE without clearing for three charge masses. The simulation displacements were within 10% of the measured maximum displacements for both types of targets.

References

[1] Randers-Pehrson G, and Bannister KA (1997). "Airblast Loading Model for DYNA2D and DYNA3D," Army Research Laboratory, Rept. ARL-TR-1310, publicly released with unlimited distribution.

[2] Hyde DW (1991) Conventional Weapons Program (ConWep). US Army Waterways Experimental Station, Vicksburg, USA.

[3] Hudson CC (1955) "Sound pulse approximations to blast loading (with comments on transient drag)," Sandia Corporation Technical Memorandum SC-TM-191-55-51 (1955). https://www.osti.gov/opennet/servlets/purl/16340913-1cPgoX/16340913.pdf. Last Accessed 27 September 2022.

[4] Tyas A, Warren J, Bennett T, and Fay S (2011). "Prediction of clearing effects in far-field blast loading of finite targets," Shock Waves, Volume 21 pages 111-119.

[5] Bogosian D, Rigby SE and Powell D (2016) "A comprehensive comparison of methods for clearing effects on reflected airblast impulse," Proceedings of the 24th Military Aspects of Blast and Shock. 24th Military Aspects of Blast and Shock (MABS), 19-23 Sep 2016, Halifax, Nova Scotia, Canada.

[6] "Structures to Resist the Effects of Accidental Explosions," U.S. Department of Defense, UFC 3-340-02, Change 2, September 2014.

[7] "Design of Blast Resistant Buildings in Petrochemical Facilities," 2nd Edition, Task Committee on Blast Resistant Design, American Society of Civil Engineers, 2010.

[8] Slavik T (2020) "LS-DYNA Keyword User Manual – Volume I." Livermore Software Technology (LST), An Ansys Company. http://ftp.lstc.com/anonymous/outgoing/jday/manuals/DRAFT_Vol_I.pdf.

[9] Rigby SE (2020) Private communication transfer of Excel files containing Tyas *et al*. experimental results and corresponding Hudson clearing results.

[10] Rigby S, Tyas A, Bennett T, Warren J and Fay S (2013). "Clearing effects on plates subjected to blast loads," Proceedings of the Institution of Civil Engineers: Engineering and Computational Mechanics, Volume 166, Issue EM3, Pages 140-148.

For further information, please contact:

Dr. Sam Rigby
University of Sheffield
E: sam.rigby@sheffield.ac.uk
W: www.sheffield.ac.uk/civil/people/academic/sam-rigby